

University of Wisconsin - Madison

MADPH-97-999

DOE-ER40757-100

KEK-TH-529

hep-ph/9707412

July 1997

## Global Study of Electron-Quark Contact Interactions

V. Barger<sup>1</sup>, Kingman Cheung<sup>2</sup>, K. Hagiwara<sup>1,3,4</sup>, and D. Zeppenfeld<sup>1</sup>

<sup>1</sup>*Physics Department, University of Wisconsin, Madison, WI 53706*

<sup>2</sup>*Center for Particle Physics, University of Texas, Austin, TX 78712*

<sup>3</sup>*Theory Group, KEK, Tsukuba, Ibaraki 305, Japan*

<sup>4</sup>*ICEPP, University of Tokyo, Hongo, Bunkyo-ku, Tokyo 113, Japan*

### Abstract

We perform a global fit of data relevant to  $eeqq$  contact interactions, including deep inelastic scattering at high  $Q^2$  from ZEUS and H1, atomic physics parity violation in Cesium from JILA, polarized  $e^-$  on nuclei scattering experiments at SLAC, Mainz and Bates, Drell-Yan production at the Tevatron, the total hadronic cross section  $\sigma_{\text{had}}$  at LEP, and neutrino-nucleon scattering from CCFR. With only the new HERA data, the presence of contact interactions improves the fit compared to the Standard Model. When other data sets are included, the size of the contact contributions is reduced and the overall fit represents no real improvement over the Standard Model.

## I. INTRODUCTION

The reports of event rates above Standard Model (SM) expectations in  $e^+p \rightarrow e^+X$  deep inelastic scattering (DIS) at very high  $Q^2$  by the H1 [1] and ZEUS [2] experiments at HERA have generated a considerable amount of theoretical activity. Various models to explain the excess events have been put forward [3–14]. Particular attention has been given to resonant production of leptoquarks [3,4], squarks with  $R$ -parity violating couplings [5,6], quark and lepton compositeness [7], and a general parametrization in terms of  $eeqq$  contact interactions [8–13], representing the exchange of very massive particles in the  $s$ ,  $t$  or  $u$ -channels.

An interest in leptoquarks derives from an indication for an  $e^+j$  invariant mass peak at  $M_{ej} \approx 200$  GeV in the H1 data. However, no clear mass peak is present in the ZEUS data; see discussion in Ref. [15]. In addition, for an  $ej$  branching fraction of unity, recent searches at the Tevatron exclude leptoquarks of mass  $M_{LQ} \leq 210$  GeV from CDF [16] and  $M_{LQ} \leq 225$  GeV from D0 [17]. The Tevatron bounds can be escaped, however, with a reduced branching fraction  $B(LQ \rightarrow ej)$ .

Any new physics in  $eq \rightarrow eq$  scattering for which the exchanged particles have mass squared  $M^2 \gg s$  can be described by an effective  $eeqq$  contact term Lagrangian. For example, effects of a  $Z'$  boson of TeV mass scale would be well represented by a four-fermion contact interaction. A leptoquark of mass  $M_{LQ} \gg 200$  GeV could similarly be described at HERA by an effective  $eeqq$  contact term. For leptoquark masses not far above the HERA energy range additional form-factor effects would have to be considered, but an analysis in terms of contact interactions would still be appropriate to derive constraints from low energy experiments.

In this paper we perform a combined analysis of low and high energy data to obtain constraints on  $eeqq$  contact interactions. The data sets include deep inelastic scattering at high  $Q^2$  from ZEUS [2] and H1 [1], atomic physics parity violation [18], polarized  $e^-$  on nuclei scattering experiments at SLAC [19], Mainz [20], and Bates [21], Drell-Yan production at the Tevatron [22], the total hadronic cross section  $\sigma_{\text{had}}$  at LEP1, LEP1.5, and LEP2 [23–27],

the left-right asymmetry  $A_{LR}$  at SLD [23], and neutrino-nucleon scattering from CCFR [28].

The organization of the paper is as follows. In Section II we discuss the parametrization of contact interactions and discuss possible symmetry relations among them. In Section III we present all the data that enter our global analysis. In Section IV we give constraints on the  $eeqq$  contact interactions in selected models and show how each experiment constrains different combinations of these interactions. Allowing for all eight  $eeuu$  and  $eedd$  contact interactions to vary freely, the high  $Q^2$  HERA data and the high mass Drell-Yan pair data from CDF cannot be fitted simultaneously. Section V gives our conclusions.

## II. PARAMETRIZATION OF CONTACT INTERACTIONS

The conventional effective Lagrangian of  $eeqq$  contact interactions has the form [29–31]

$$L_{NC} = \sum_q \left[ \eta_{LL} (\bar{e}_L \gamma_\mu e_L) (\bar{q}_L \gamma^\mu q_L) + \eta_{RR} (\bar{e}_R \gamma_\mu e_R) (\bar{q}_R \gamma^\mu q_R) \right. \\ \left. + \eta_{LR} (\bar{e}_L \gamma_\mu e_L) (\bar{q}_R \gamma^\mu q_R) + \eta_{RL} (\bar{e}_R \gamma_\mu e_R) (\bar{q}_L \gamma^\mu q_L) \right], \quad (1)$$

where the eight independent coefficients  $\eta_{\alpha\beta}^{eu}$  and  $\eta_{\alpha\beta}^{ed}$  have dimension  $(\text{TeV})^{-2}$  and are conventionally expressed as  $\eta_{\alpha\beta}^{eq} = \epsilon g^2 / \Lambda_{eq}^2$ , with a fixed  $g^2 = 4\pi$ . The sign factor  $\epsilon = \pm 1$  allows for either constructive or destructive interference with the SM  $\gamma$  and  $Z$  exchange amplitudes and  $\Lambda_{eq}$  represents the mass scale of the exchanged new particles, with coupling strength  $g^2/4\pi = 1$ . A coupling of this order is expected in substructure models and therefore  $\Lambda_{eq}$  is sometimes called the “compositeness scale” [29]. In the effective interaction (1) we do not include lepton or quark chirality violating terms such as  $(\bar{e}_L e_R) (\bar{q}_L q_R)$  since, if there is an approximate  $SU(2) \times U(1)$  invariance, scalar and tensor contact terms are severely constrained by helicity suppressed processes like  $\pi^- \rightarrow e^- \bar{\nu}$  [3]. A contact term Lagrangian completely analogous to Eq. (1) can be written down for  $\nu\nu qq$  interactions, with parameters  $\eta_{LL}^{\nu q}$  and  $\eta_{LR}^{\nu q}$ , respectively.

### A. $SU(2) \times U(1)$ symmetry and universality

Left-handed electrons and quarks belong to  $SU(2)$  doublets  $L = (\nu_L, e_L)$  and  $Q = (u_L, d_L)$  and thus from  $SU(2)$  symmetry one expects relations between contact terms involving left-handed  $u$  or  $d$  quarks; similarly, contact terms for left-handed electrons and neutrinos should be related [12]. In order to exhibit these relationships we start from the most general  $SU(2) \times U(1)$  invariant contact term Lagrangian,

$$\begin{aligned} \mathcal{L}_{SU(2)} = & \eta_1 (\bar{L}\gamma^\mu L) (\bar{Q}\gamma_\mu Q) + \eta_2 (\bar{L}\gamma^\mu T^a L) (\bar{Q}\gamma_\mu T^a Q) + \eta_3 (\bar{L}\gamma^\mu L) (\bar{u}_R\gamma_\mu u_R) \\ & + \eta_4 (\bar{L}\gamma^\mu L) (\bar{d}_R\gamma_\mu d_R) + \eta_5 (\bar{e}_R\gamma^\mu e_R) (\bar{Q}\gamma_\mu Q) + \eta_6 (\bar{e}_R\gamma^\mu e_R) (\bar{u}_R\gamma_\mu u_R) \\ & + \eta_7 (\bar{e}_R\gamma^\mu e_R) (\bar{d}_R\gamma_\mu d_R) . \end{aligned} \quad (2)$$

Here we have suppressed the lepton chirality violating term  $(\bar{L}\gamma^\mu Q) (\bar{d}_R\gamma_\mu e_R)$  which, under a Fierz transformation, is equivalent to a  $(\bar{L}e_R) (\bar{d}_R Q)$  term which, as noted before, is severely constrained by  $\pi^- \rightarrow e^- \bar{\nu}$  data. In the second term of Eq. (2)  $T^a = \sigma^a/2$  denotes the  $SU(2)$  generators; this term describes the exchange of isospin triplet quanta between the lepton and quark fields. Because of this possible contribution no constraints arise for the  $\eta_{LL}^{eq}$  contact terms and the difference  $\eta_{LL}^{ed} - \eta_{LL}^{eu} = \eta_2/2$  measures the size of  $evud$  contact terms in CC processes.  $SU(2)$  does constrain right-handed electron couplings,

$$\eta_{RL}^{eu} = \eta_5 = \eta_{RL}^{ed} . \quad (3)$$

In addition, the four neutrino and the lepton couplings are related by  $SU(2)$ ,

$$\begin{aligned} \eta_{LL}^{\nu u} &= \eta_1 + \frac{1}{4}\eta_2 = \eta_{LL}^{ed} , \\ \eta_{LL}^{\nu d} &= \eta_1 - \frac{1}{4}\eta_2 = \eta_{LL}^{eu} , \\ \eta_{LR}^{\nu u} &= \eta_3 = \eta_{LR}^{eu} , \\ \eta_{LR}^{\nu d} &= \eta_4 = \eta_{LR}^{ed} . \end{aligned} \quad (4)$$

In our analyses, the relations of Eqs. (3) and (4) are only used when neutrino scattering data are included in the analysis. Even though we expect that  $SU(2) \times U(1)$  will be a

symmetry of the renormalizable interactions which ultimately manifest themselves as the contact terms of Eq. (1), electroweak symmetry breaking may break the degeneracy of SU(2) multiplets of new, heavy quanta whose exchanges give rise to (1). This would result in a violation of the relations of Eqs. (3) and (4). One example is the exchange of the stop  $\tilde{t}_1$ ,  $\tilde{t}_2$ , and the sbottom  $\tilde{b}_L, \tilde{b}_R$  in  $R$ -parity violating SUSY models. The large top-quark mass may lead to substantial splitting of the masses of these squarks which could easily lead to violations by up to a factor of two of SU(2) relations such as  $\eta_{LR}^{\nu d} = \eta_{LR}^{ed}$ .

In the discussion above we have considered first generation quarks and leptons only, because the ‘‘HERA anomaly’’ raises particular interest in such couplings. In principle, all  $\eta$ ’s carry four independent generation indices and may give rise to other flavor conserving and flavor changing transitions. Because of severe experimental constraints on intragenerational transitions [32] like  $K \rightarrow \mu e$  we restrict our discussion to first generation contact terms. Only where required by particular data (e.g. the LEP data which sum over the quarks of all three generations) will we assume universality of contact terms between  $e, \mu$  and  $\tau$  and up- and down-type quarks of different generations.

Other symmetry constraints on the parametrization of four-fermion contact interactions are of interest as well:

- i) SU(12) symmetry considerations [9] give

$$\eta_{\alpha L}^{eq} = -\eta_{\alpha R}^{eq}, \quad \alpha = L \text{ or } R. \quad (5)$$

In addition, SU(2)<sub>L</sub> gauge invariance requires the  $u$ -quark contribution equal to the  $d$ -quark contribution, i.e.,

$$\eta_{\alpha L}^{eu} = \eta_{\alpha L}^{ed}, \quad \alpha = L \text{ or } R. \quad (6)$$

With these symmetries the atomic parity violation constraint is satisfied naturally.

- ii) Vector-vector (VV) interactions [10], from the exchange of a boson with purely vector couplings, give

$$\eta_{LL}^{eq} = \eta_{RR}^{eq} = \eta_{LR}^{eq} = \eta_{RL}^{eq} \equiv \eta_{VV}^{eq} . \quad (7)$$

iii) Axial-axial interactions [10,11], from the exchange of purely axial-vector couplings, give

$$\eta_{LL}^{eq} = \eta_{RR}^{eq} = -\eta_{LR}^{eq} = -\eta_{RL}^{eq} \equiv \eta_{AA}^{eq} . \quad (8)$$

We consider fits with these restrictions imposed subsequently to make model-independent analysis.

## B. Observables and four-fermion amplitudes

All the observables that we consider are described by a four-fermion  $S$ -matrix element. The amplitudes for observables such as  $e^+e^- \rightarrow$  hadrons,  $p\bar{p} \rightarrow \ell^+\ell^-X$  and atomic parity violation, are obtained from the amplitude for  $eq \rightarrow eq$  scattering by crossing; they are given by angular factors times reduced amplitudes  $M_{\alpha\beta}^{eq}$ , where the subscripts label the chiralities of the initial lepton ( $\alpha$ ) and quark ( $\beta$ ). The SM tree level reduced amplitude for  $eq \rightarrow eq$  is

$$M_{\alpha\beta}^{eq}(\hat{t}) = -\frac{e^2 Q_q}{\hat{t}} + \frac{e^2}{\sin^2 \theta_w \cos^2 \theta_w} \frac{g_\alpha^e g_\beta^q}{\hat{t} - m_Z^2}, \quad \alpha, \beta = L, R \quad (9)$$

where  $\hat{t} = -Q^2$  is the Mandelstam variable,  $g_L^f = T_{3f} - \sin^2 \theta_w Q_f$  and  $g_R^f = -\sin^2 \theta_w Q_f$ ,  $T_{3f}$  and  $Q_f$  are, respectively, the third component of the SU(2) isospin and the electric charge of the fermion  $f$  in units of the proton charge, and  $e^2 = 4\pi\alpha_{\text{em}}$ . For  $e^+e^- \rightarrow q\bar{q}$  or  $q\bar{q} \rightarrow e^+e^-$ , the amplitude  $M_{\alpha\beta}^{eq}(\hat{s})$  is obtained from Eq. (9) with the replacement  $\hat{t} \rightarrow \hat{s}$  and  $\hat{t} - M_Z^2 \rightarrow \hat{s} - M_Z^2 + i\hat{s}\Gamma_Z/M_Z$ , where  $\hat{s}$  is the subprocess c.m. energy squared. The new physics contributions to the reduced amplitudes  $M_{\alpha\beta}$  from the  $eeqq$  contact interactions of Eq. (1) are

$$\Delta M_{\alpha\beta}^{eq} = \eta_{\alpha\beta}^{eq}, \quad \alpha, \beta = L, R . \quad (10)$$

### C. Contributions to Standard Model parameters

In low energy neutral current (NC) processes, at  $\sqrt{s} \ll m_Z^2$ ,  $Z$  boson exchange can also be described by effective four-fermion contact terms. For the parity violating contributions to  $eeqq$  NC interactions the NC Lagrangian is conventionally expressed in terms of parameters  $C_{1q}$  and  $C_{2q}$  as

$$\mathcal{L}^{e\text{Hadron}} = \frac{G_F}{\sqrt{2}} \sum_q \left[ C_{1q} (\bar{e}\gamma^\mu\gamma^5 e) (\bar{q}\gamma_\mu q) + C_{2q} (\bar{e}\gamma^\mu e) (\bar{q}\gamma_\mu\gamma^5 q) \right]. \quad (11)$$

The radiatively corrected SM values are [33]

$$\begin{aligned} C_{1q}^{\text{SM}} &= \rho'_{eq} \left[ -T_{3q} + 2Q_q (\kappa'_{eq} \sin^2 \theta_w) \right], \\ C_{2q}^{\text{SM}} &= -T_{3q} \rho_{eq} \left[ 1 - 4 (\kappa_{eq} \sin^2 \theta_w) \right] + \lambda_{2q}, \end{aligned} \quad (12)$$

where  $\sin^2 \theta_w = 0.2236$ ,  $\rho'_{eq} = 0.9884$  and  $\kappa'_{eq} = 1.036$  for the atomic parity violation experiments while  $\rho'_{eq} = 0.979$ ,  $\kappa'_{eq} = 1.034$ ,  $\rho_{eq} = 1.002$ ,  $\kappa_{eq} = 1.06$ ,  $\lambda_{2u} = -0.013$ , and  $\lambda_{2d} = 0.003$  for the lepton-nucleon scattering. The contact term Lagrangian introduces parameter shifts

$$\begin{aligned} \Delta C_{1q} &= \frac{1}{2\sqrt{2}G_F} \left[ -\eta_{LL}^{eq} + \eta_{RR}^{eq} - \eta_{LR}^{eq} + \eta_{RL}^{eq} \right], \\ \Delta C_{2q} &= \frac{1}{2\sqrt{2}G_F} \left[ -\eta_{LL}^{eq} + \eta_{RR}^{eq} + \eta_{LR}^{eq} - \eta_{RL}^{eq} \right], \quad q = u, d \end{aligned} \quad (13)$$

that can be constrained by experimental data on atomic parity violation and electron nucleon scattering.

If  $SU(2) \times U(1)$  is a good symmetry of the contact interactions then neutrino-nucleon scattering data also constrain the  $eeqq$  contact terms [12]. Comparing to the conventional parametrization of neutrino-quark effective interactions,

$$\mathcal{L} = -\frac{G_F}{\sqrt{2}} \bar{\nu}\gamma^\mu(1-\gamma_5)\nu \sum_q \left[ g_L^q \bar{q}\gamma_\mu(1-\gamma_5)q + g_R^q \bar{q}\gamma_\mu(1+\gamma_5)q \right], \quad (14)$$

the contact interactions (1) introduce shifts in the coefficients  $g_{L,R}^q$ ,

$$\Delta g_L^q = -\frac{1}{2\sqrt{2}G_F} \eta_{LL}^{eq}, \quad \Delta g_R^q = -\frac{1}{2\sqrt{2}G_F} \eta_{LR}^{eq}, \quad q = u, d. \quad (15)$$

Here we have used the  $SU(2) \times U(1)$  relations of Eq. (4). The SM values for these couplings are [33]

$$(g_L^q)^{\text{SM}} = 1.0095 \left( T_{3q} - Q_q (1.0382 \sin^2 \theta_w) + \lambda_{qL} \right) \quad (16)$$

$$(g_R^q)^{\text{SM}} = 1.0095 \left( -Q_q (1.0382 \sin^2 \theta_w) + \lambda_{qR} \right), \quad (17)$$

with  $\lambda_{uL} = -0.0032$ ,  $\lambda_{dL} = -0.0026$  and  $\lambda_{uR} = \lambda_{dR}/2 = 3.6 \times 10^{-5}$ .

### D. Connection to specific models

A second  $Z$ -boson,  $Z_2$ , of mass  $M_{Z_2}$  and with chiral couplings  $eg_\alpha^{f(2)}$  to fermion species  $f$ , would give rise to four-fermion contact terms with

$$\eta_{\alpha\beta}^{eq} = -e^2 \frac{g_\alpha^{e(2)} g_\beta^{q(2)}}{M_{Z_2}^2}, \quad (18)$$

in experiments at  $\hat{s} \ll M_{Z_2}^2$ . For subprocess energies of the order of the  $Z_2$  mass, as may be achievable at the Tevatron, form-factor effects, due to the  $\hat{s}$  dependence of the  $Z_2$  propagator, would have to be considered.

The exchange of scalar leptoquarks would give rise to contact terms

$$\eta_{\alpha\beta}^{eu} = e^2 \left( \frac{h_{2L}^2 \delta_{\alpha L} \delta_{\beta R}}{2(-M_{R_{2L}}^2)} + \frac{h_{2R}^2 \delta_{\alpha R} \delta_{\beta L}}{2(-M_{R_{2R}}^2)} \right), \quad \eta_{\alpha\beta}^{ed} = e^2 \left( \frac{\tilde{h}_{2L}^2 \delta_{\alpha L} \delta_{\beta R}}{2(-M_{\tilde{R}_{2L}}^2)} + \frac{h_{2R}^2 \delta_{\alpha R} \delta_{\beta L}}{2(-M_{R_{2R}}^2)} \right). \quad (19)$$

where  $eh_{2L}, eh_{2R}, e\tilde{h}_{2L}$  are the couplings of  $R_{2L}, R_{2R}, \tilde{R}_{2L}$ , respectively [34]. A leptoquark mass in the 200–300 GeV range would again necessitate the inclusion of form-factor (propagator) effects in the analysis of HERA and Tevatron data. For the low-energy data, however, the contact term parametrization would be entirely adequate.

## III. EXPERIMENTAL DATA SETS

### A. ZEUS and H1: $e^+p \rightarrow e^+X$

The H1 and ZEUS experiments have provided cross section measurements in  $x, y$  bins where  $x$  and  $y$  are the usual scaling variables of DIS:

$$x = Q^2/[2p \cdot (k - k')], \quad y = Q^2/[sx]. \quad (20)$$

Here  $k$  and  $k'$  are the four-momenta of the incoming electron and outgoing positron, respectively,  $p$  is the proton four-momentum,  $s \simeq (300 \text{ GeV})^2$  is the square of the c.m. energy, and  $Q^2$  is the square of the momentum transfer

$$Q^2 = -(k - k')^2 = sxy. \quad (21)$$

The observed distribution of events in  $x, y$  bins is given in Table I for ZEUS [2] and in Table II for H1 [1], along with SM expectations that include experimental efficiencies.

Neutral current deep inelastic scattering occurs via the subprocess  $eq \rightarrow eq$ . In terms of the reduced amplitudes  $M_{\alpha\beta}^{eq}(\hat{t})$  ( $\alpha, \beta = L, R$ ) of Eq. (9) the spin- and color-averaged amplitude-squared for  $e^+(k)q(p) \rightarrow e^+(k')q(p')$  is given by

$$\overline{|\mathcal{M}(e^+q \rightarrow e^+q)|^2} = \left( |M_{LL}^{eq}(\hat{t})|^2 + |M_{RR}^{eq}(\hat{t})|^2 \right) \hat{u}^2 + \left( |M_{LR}^{eq}(\hat{t})|^2 + |M_{RL}^{eq}(\hat{t})|^2 \right) \hat{s}^2, \quad (22)$$

where  $\hat{t} = -sxy$ ,  $\hat{u} = -sx(1 - y)$  and  $\hat{s} = sx$ . In our analysis we calculate the SM tree level cross section for each  $x, y$  bin. We then compare with the efficiency corrected SM results in Tables I and II to obtain correction factors for each bin,

$$C(x, y) = \frac{\sigma^{\text{SM}}(x, y; \text{corrected})}{\sigma^{\text{SM}}(x, y)} \quad (23)$$

Then in analyzing models that include new physics contributions we multiply the theoretical cross sections by  $C(x, y)$  to take into account the experimental efficiencies and compare the corrected result with the observed cross section.. We treat the H1 and ZEUS data separately.

The SM DIS differential cross section is given by

$$\begin{aligned} \frac{d\sigma(e^+p)}{dx dy} = & \frac{sx}{16\pi} \left\{ u(x, Q^2) \left[ |M_{LR}^{eu}(\hat{t})|^2 + |M_{RL}^{eu}(\hat{t})|^2 + (1 - y)^2 \left( |M_{LL}^{eu}(\hat{t})|^2 + |M_{RR}^{eu}(\hat{t})|^2 \right) \right] \right. \\ & + d(x, Q^2) \left[ |M_{LR}^{ed}(\hat{t})|^2 + |M_{RL}^{ed}(\hat{t})|^2 + (1 - y)^2 \left( |M_{LL}^{ed}(\hat{t})|^2 + |M_{RR}^{ed}(\hat{t})|^2 \right) \right] \\ & + \bar{u}(x, Q^2) \left[ |M_{LL}^{eu}(\hat{t})|^2 + |M_{RR}^{eu}(\hat{t})|^2 + (1 - y)^2 \left( |M_{LR}^{eu}(\hat{t})|^2 + |M_{RL}^{eu}(\hat{t})|^2 \right) \right] \\ & \left. + \bar{d}(x, Q^2) \left[ |M_{LL}^{ed}(\hat{t})|^2 + |M_{RR}^{ed}(\hat{t})|^2 + (1 - y)^2 \left( |M_{LR}^{ed}(\hat{t})|^2 + |M_{RL}^{ed}(\hat{t})|^2 \right) \right] \right\} \end{aligned}$$

$$\begin{aligned}
& +s(x, Q^2) \left[ |M_{LR}^{es}(\hat{t})|^2 + |M_{RL}^{es}(\hat{t})|^2 + (1-y)^2 \left( |M_{LL}^{es}(\hat{t})|^2 + |M_{RR}^{es}(\hat{t})|^2 \right) \right] \\
& +\bar{s}(x, Q^2) \left[ |M_{LL}^{es}(\hat{t})|^2 + |M_{RR}^{es}(\hat{t})|^2 + (1-y)^2 \left( |M_{LR}^{es}(\hat{t})|^2 + |M_{RL}^{es}(\hat{t})|^2 \right) \right] \\
& +c(x, Q^2) \left[ |M_{LR}^{ec}(\hat{t})|^2 + |M_{RL}^{ec}(\hat{t})|^2 + (1-y)^2 \left( |M_{LL}^{ec}(\hat{t})|^2 + |M_{RR}^{ec}(\hat{t})|^2 \right) \right] \\
& +\bar{c}(x, Q^2) \left[ |M_{LL}^{ec}(\hat{t})|^2 + |M_{RR}^{ec}(\hat{t})|^2 + (1-y)^2 \left( |M_{LR}^{ec}(\hat{t})|^2 + |M_{RL}^{ec}(\hat{t})|^2 \right) \right] \Big\} , \quad (24)
\end{aligned}$$

where  $u(x, Q^2)$ ,  $d(x, Q^2)$  etc. are parton distributions.

## B. Atomic Parity Violation Experiment

Parity violation in the SM is due to exchanges of weak gauge bosons, with vector-axial-vector ( $VA$ ) and axial-vector-vector ( $AV$ ) terms contributing. Atomic physics parity violation measures [35] electron-quark couplings that are different than those probed by high energy experiments and thereby provides alternative constraints on new physics. In terms of the coefficients  $C_{1q}$  and  $C_{2q}$  of the NC Lagrangian (11), the weak charge  $Q_W$  of a heavy atom is given by [35]

$$Q_W = -2 \left[ C_{1u}(2Z + N) + C_{1d}(Z + 2N) \right] , \quad (25)$$

where  $Z$  and  $N$  are the number of protons and neutrons respectively in the nucleus of the atom. Recently a very precise measurement was made of the parity violation transition between the 6S and 7S states of Cesium with the use of a spin-polarized atomic beam [18]. For  $^{133}_{55}\text{Cs}$ ,  $Q_w \equiv -376C_{1u} - 422C_{1d}$ . The weak charge  $Q_W$  of the atom was determined to be

$$Q_W^{\text{exp}} = -72.11 \pm 0.27 \pm 0.89 , \quad (26)$$

where the first uncertainty is experimental and the second is theoretical. The new measurement of (26) represents substantial improvement from the value given in the 1996 Particle Data Book [33] and shows better agreement with the SM value. Including radiative corrections the predicted SM value for Cs is [36]

$$Q_W^{\text{SM}} = -73.11 \pm 0.05. \quad (27)$$

We find the following constraint for the new physics contribution

$$\Delta Q_W(Cs) = -376\Delta C_{1u} - 422\Delta C_{1d} = 1.00 \pm 0.93. \quad (28)$$

Some chirality combinations of  $LL, RR, LR, RL$  give zero contributions to  $\Delta C_{1q}$  and thus satisfy the experimental  $Q_W$  constraint. Such possibilities include (i)  $LL = RR = LR = RL$  ( $VV$ ), (ii)  $LL = RR = -LR = -RL$  ( $AA$ ), (iii)  $LL = -LR, RL = -RR$  (an  $SU(12)$  symmetry [9]), (iv)  $LR = RL, LL = RR = 0$  (a minimal choice used in fitting the HERA data [8]).

### C. Polarization Asymmetries in Electron-Nucleus Scattering Experiment

In this subsection, we review three experiments on polarized electron-nucleus scattering: the SLAC  $e$ -D scattering experiment [19], the Mainz  $e$ -Be scattering experiment [20], and the Bates  $e$ -C scattering experiment [21].

#### 1. SLAC $e$ -D experiment

The SLAC polarized  $e$ -D experiment [19] measured the parity-violating asymmetry

$$A = \frac{d\sigma_R - d\sigma_L}{d\sigma_R + d\sigma_L}, \quad (29)$$

where  $d\sigma_{R/L}$  are the differential cross sections for  $e_{R/L}^- D \rightarrow eX$  scattering. At low energy  $A$  is given in the valence approximation to the parton model by [33,35]

$$\frac{A}{Q^2} = \frac{3G_F}{5\sqrt{2}\pi\alpha_{\text{em}}} \left[ \left( C_{1u} - \frac{C_{1d}}{2} \right) + \left( C_{2u} - \frac{C_{2d}}{2} \right) \frac{1 - (1-y)^2}{1 + (1-y)^2} \right], \quad (30)$$

where  $Q^2 > 0$  is the momentum transfer,  $y$  is the fractional energy transfer from the electron to hadrons, and  $C_{1q}, C_{2q}$  are the coefficients of the parity-violating Lagrangian in Eq. (11). After taking into account uncertainties in the sea-quark contribution, the  $R = \sigma_L/\sigma_R$  ratio and the higher-twist effects, the following constraints are found [37]

$$2C_{1u} - C_{1d} = -0.94 \pm 0.26, \quad 2C_{2u} - C_{2d} = 0.66 \pm 1.23, \quad \rho_{\text{corr}} = -0.975, \quad (31)$$

where  $\rho_{\text{corr}}$  is the correlation. The recent update of the SM contribution to the effective parameters at  $\langle Q^2 \rangle \simeq 1.5 \text{ GeV}^2$  finds [36]

$$(2C_{1u} - C_{1d})^{\text{SM}} = -0.723 \pm 0.005, \quad (32a)$$

$$(2C_{2u} - C_{2d})^{\text{SM}} = 0.105 \pm 0.006. \quad (32b)$$

We hence use the following constraints for the new physics contributions

$$\Delta(2C_{1u}^e - C_{1d}^e) = -0.22 \pm 0.26, \quad \Delta(2C_{2u}^e - C_{2d}^e) = 0.77 \pm 1.23, \quad \rho_{\text{corr}} = -0.975. \quad (33)$$

Note the strong negative correlation of the errors.

## *2. Mainz e-Be experiment*

At Mainz, asymmetry of quasi-elastic polarized electron scattering on a  $^9\text{Be}$  target has been measured [20]. The experiment was performed at the mean momentum transfer  $\langle Q^2 \rangle \simeq 0.2025 \text{ GeV}^2$ . The measured asymmetry parameter  $A_{\text{Mainz}}$  is given by the following combination of the coefficients of the effective Lagrangian (11)

$$A_{\text{Mainz}} = 2.73C_{1u} - 0.65C_{1d} + 2.19C_{2u} - 2.03C_{2d}, \quad (34)$$

and the experimental result is

$$A_{\text{Mainz}} = -0.94 \pm 0.19. \quad (35)$$

Here the error is obtained by taking the quadratic sum of the theoretical and experimental errors as quoted in Ref. [20].

The theoretical prediction in the SM has been evaluated in [36] to be

$$A_{\text{Mainz}}^{\text{SM}} = -0.875 \pm 0.014. \quad (36)$$

We hence find the following constraint on new physics contribution

$$\begin{aligned} \Delta A_{\text{Mainz}} &= 2.73\Delta C_{1u}^e - 0.65\Delta C_{1d}^e + 2.19\Delta C_{2u}^e - 2.03\Delta C_{2d}^e \\ &= -0.065 \pm 0.19. \end{aligned} \quad (37)$$

### 3. Bates $e$ -C experiment

The asymmetry of elastic polarized electrons scattering on a  $^{12}\text{C}$  target has been measured at Bates [21]. Their asymmetry parameter can be expressed in terms of the effective Lagrangian coefficients as follows;

$$A_{\text{Bates}} = \frac{3\sqrt{2}G_F Q^2}{4\pi\alpha(-Q^2)}(C_{1u} + C_{1d}). \quad (38)$$

The typical momentum transfer of the experiment is small,  $\langle Q^2 \rangle = 0.0225 \text{ GeV}^2$ , and contributions from quarks other than the  $u$  and  $d$  quarks can be safely neglected [38]. From the measurement [21]

$$A_{\text{Bates}} = (1.62 \pm 0.38) \times 10^{-6}, \quad (39)$$

and the estimate [39]  $1/\alpha(-0.0225 \text{ GeV}^2) = 135.87$ , we obtain the following constraint on the effective Lagrangian coefficients,

$$C_{1u} + C_{1d} = 0.137 \pm 0.033. \quad (40)$$

The theoretical prediction of the SM at  $\langle Q^2 \rangle = 0.0225 \text{ GeV}^2$  is [36]

$$(C_{1u} + C_{1d})^{\text{SM}} = 0.1522 \pm 0.0004. \quad (41)$$

Therefore the constraint on new physics is

$$\Delta(C_{1u}^e + C_{1d}^e) = -0.0152 \pm 0.033. \quad (42)$$

### D. CDF Drell-Yan Cross Sections

The CDF experiment at the Tevatron has reported preliminary data [22] on Drell-Yan lepton-pair production. The data that we use in our analysis are extracted from a CDF figure; the values are given in Table III. The data are differential cross sections versus  $M$ , integrated over  $|y| < 1$  and divided by two to average over rapidity, where  $M$  and  $y$  are,

respectively, the invariant mass and rapidity of the lepton pair. The double differential cross section versus  $M$  and  $y$  of the lepton pair is given by

$$\frac{d^2\sigma}{dMdy} = K \frac{M^3}{72\pi s} \sum_q q(x_1)\bar{q}(x_2) \left[ |M_{LL}^{eq}(\hat{s})|^2 + |M_{RR}^{eq}(\hat{s})|^2 + |M_{LR}^{eq}(\hat{s})|^2 + |M_{RL}^{eq}(\hat{s})|^2 \right], \quad (43)$$

where  $q(x)$  and  $\bar{q}(x)$  are parton distributions evaluated at  $Q^2 = M^2$ ,  $x_{1,2} = Me^{\pm y}/\sqrt{s}$ ,  $\sqrt{s} = 1800$  GeV, and  $\hat{s} = M^2$ . The reduced amplitudes  $M_{\alpha\beta}^{eq}(\hat{s})$  are given by Eq. (9) with  $\hat{t}$  replaced by  $\hat{s}$ . The QCD  $K$ -factor of Drell-Yan production is given by [40]

$$K = 1 + \frac{\alpha_s(M^2)}{2\pi} \frac{4}{3} \left( 1 + \frac{4}{3}\pi^2 \right). \quad (44)$$

With this  $K$  factor, the overall cross section normalization agrees with the CDF data in the vicinity of the  $Z$ -peak.

### E. $e^+e^-$ Experiments

The  $eeqq$  contact interactions probed at HERA and in low energy experiments involve only light quarks. In  $e^+e^- \rightarrow$  hadrons both light and heavy quarks contribute and separation of the light quark contributions requires bottom and charm quark tagging. To investigate the influence of contact terms on  $e^+e^- \rightarrow$  hadrons we assume here that the  $eeqq$  contact interaction is flavor independent. The relevant measurements are the total hadronic cross sections  $\sigma_{\text{had}}$  and the left-right asymmetry  $A_{LR}$  at LEP1 and SLD and  $\sigma_{\text{had}}$  at LEP1.5 and LEP2. Our analysis is based on the data in Refs. [23–27].

At leading order in the electroweak interactions the total hadronic cross section summed over all flavors  $q = u, d, s, c, b$  is

$$\sigma_{\text{had}} = K \sum_q \frac{s}{16\pi} \left[ |M_{LL}^{eq}(s)|^2 + |M_{RR}^{eq}(s)|^2 + |M_{LR}^{eq}(s)|^2 + |M_{RL}^{eq}(s)|^2 \right], \quad (45)$$

where the QCD  $K$  factor is given by  $K = 1 + \alpha_s/\pi + 1.409(\alpha_s/\pi)^2 - 12.77(\alpha_s/\pi)^3$  [41]. The left-right asymmetry  $A_{LR}$  is given by

$$A_{LR} = \frac{\sigma_L - \sigma_R}{\sigma_L + \sigma_R} = \frac{\sum_q (|M_{LL}^{eq}(s)|^2 + |M_{LR}^{eq}(s)|^2 - |M_{RL}^{eq}(s)|^2 - |M_{RR}^{eq}(s)|^2)}{\sum_q (|M_{LL}^{eq}(s)|^2 + |M_{LR}^{eq}(s)|^2 + |M_{RL}^{eq}(s)|^2 + |M_{RR}^{eq}(s)|^2)}. \quad (46)$$

At  $\sqrt{s} = M_Z$ , the SM amplitudes are imaginary whereas contact term contributions are real. Because of the absence of interference with the SM amplitudes, the  $Z$ -pole data have little sensitivity to the contact terms despite their high accuracy. To take into account next-to-leading order (NLO) electroweak radiative corrections we calculate

$$\sigma_{\text{had}}^{\text{theory}} = \sigma_{\text{LO}}^{\text{theory}} \times \left( \frac{\sigma_{\text{NLO}}^{\text{SM}}}{\sigma_{\text{LO}}^{\text{SM}}} \right), \quad (47)$$

where  $\sigma_{\text{LO}}^{\text{theory}}$  is given by (45) with contact interaction contributions included in the matrix elements. Table IV gives the measured  $\sigma_{\text{had}}$  and the calculated values of  $\sigma_{\text{NLO}}^{\text{SM}}$ . The radiative corrections to the LR asymmetry cancel in the ratio (46) so here we compare the observed  $A_{LR}$  with the leading order SM calculation. The experimental and the SM predicted values for  $A_{LR}$  are [23]

$$A_{LR}^{\text{exp}} = 0.1542 \pm 0.0037, \quad A_{LR}^{\text{SM}} = 0.145 \pm 0.001 \pm 0.001. \quad (48)$$

Other LEP1.5 and LEP2 measurements are summarized in Table IV. The new physics contributions are given by Eq. (10).

## F. Neutrino-Nucleon DIS Experiments

Deep inelastic scattering (DIS) experiments with neutrino and anti-neutrino beams have provided important tests for the SM since the early 80's [42,43]. If  $SU(2)_L$  invariance is assumed, then  $\nu N$  DIS data also constrain contact interactions. The CCFR collaboration obtained a model-independent constraint on the effective  $\nu\nu qq$  couplings [28]:

$$\kappa = 0.5820 \pm 0.0041 = 1.7897g_L^2 + 1.1479g_R^2 - 0.0916\delta_L^2 - 0.0782\delta_R^2, \quad (49)$$

where  $g_{L,R}^2 = (g_{L,R}^u)^2 + (g_{L,R}^d)^2$ ,  $\delta_{L,R}^2 = (g_{L,R}^u)^2 - (g_{L,R}^d)^2$  and  $g_L^q, g_R^q$  are the coefficients of the effective Lagrangian (14). The Standard Model value is  $\kappa = \kappa_{\text{SM}} = 0.5817 \pm 0.0013$  [28]. This model-independent constraint (49) can be used to constrain physics beyond the SM. Since this CCFR result is so far the most accurate measurement for  $\nu N$  scattering, we adopt their result in our analysis. We can write  $g_L^u = (g_L^u)_{\text{SM}} + \Delta g_L^u$ , etc., then  $\kappa$  becomes

$$\begin{aligned}
\kappa &= \kappa_{\text{SM}} + 1.7897 \left( 2(g_L^u)_{\text{SM}} \Delta g_L^u + (\Delta g_L^u)^2 + 2(g_L^d)_{\text{SM}} \Delta g_L^d + (\Delta g_L^d)^2 \right) \\
&+ 1.1479 \left( 2(g_R^u)_{\text{SM}} \Delta g_R^u + (\Delta g_R^u)^2 + 2(g_R^d)_{\text{SM}} \Delta g_R^d + (\Delta g_R^d)^2 \right) \\
&- 0.0916 \left( 2(g_L^u)_{\text{SM}} \Delta g_L^u + (\Delta g_L^u)^2 - 2(g_L^d)_{\text{SM}} \Delta g_L^d - (\Delta g_L^d)^2 \right) \\
&- 0.0782 \left( 2(g_R^u)_{\text{SM}} \Delta g_R^u + (\Delta g_R^u)^2 - 2(g_R^d)_{\text{SM}} \Delta g_R^d - (\Delta g_R^d)^2 \right) , \tag{50}
\end{aligned}$$

where the  $\Delta g_{L,R}^{u,d}$  are the contact term contributions of Eq. (15).

### G. Statistical Analysis

The method of maximum likelihood is the most general method of parameter estimation. For a set of independently measured quantities  $x_i$  that come from a probability density function  $f(x; \alpha)$ , where  $\alpha$  is a set of unknown parameters, the method of maximum likelihood consists of finding the set of  $\hat{\alpha}$ , which maximizes the joint probability density for all data, given by the likelihood function  $\mathcal{L} = \prod_i f(x_i; \alpha)$ . Very often it is easier to maximize the logarithm of this likelihood function by solving the equation  $\partial \log \mathcal{L} / \partial \alpha = 0$ . In the case of ZEUS and H1 data, since the number of observed events in each bin is small, it is appropriate to describe the probabilities of the observed events using Poisson statistics:

$$f_i = \frac{(n_i^{\text{th}})^{n_i^{\text{obs}}} e^{-n_i^{\text{th}}}}{n_i^{\text{obs}}!} , \tag{51}$$

where  $n_i^{\text{th}}$  is the expected number of events from the theory and  $n_i^{\text{obs}}$  is the number of observed events in the  $i$ th bin. With Poisson statistics the method of maximum log-likelihood is equivalent to minimizing the following  $\chi^2$  [33]

$$\chi^2 = \sum_i \left[ 2(n_i^{\text{th}} - n_i^{\text{obs}}) + 2n_i^{\text{obs}} \log \left( \frac{n_i^{\text{obs}}}{n_i^{\text{th}}} \right) \right] . \tag{52}$$

In the bins where  $n_i^{\text{obs}} = 0$  the second term is zero. In our fitting procedures, we shall vary unknown  $n$  parameters of the contact interaction and calculate the expected number of events,  $n_i^{\text{th}}$ , for each bin  $i$ ; then we obtain the quantity  $\chi^2$  for all relevant ranges of the unknown parameters. The set of parameters that gives the minimum  $\chi^2$  value is the best

estimate of the parameters. Relative merits of different new physics interactions can also be compared by their  $\chi^2$  values.

In experiments with good statistics, we use the usual approach to calculate

$$\chi^2 = \sum_{i=\text{bins or data points}} \left( \frac{x_i^{\text{exp}} - x_i^{\text{th}}}{\sigma_{x_i}} \right)^2, \quad (53)$$

where  $x_i^{\text{exp}}$ ,  $x_i^{\text{th}}$ , and  $\sigma_{x_i}$  are the experimental measurements, theoretical predictions, and the errors, respectively. The method of maximum log likelihood is equivalent to the usual  $\chi^2$  method when the distribution follows Gaussian statistics. The  $\chi^2$ 's from all data sets are added together to form the total  $\chi^2$  and best estimate  $\hat{\alpha}$  for the set of parameters is obtained by minimizing the total  $\chi^2$ , i.e.,  $\chi^2(\hat{\alpha}) = \chi_{\text{min}}^2$ . The  $n$ -sigma standard deviation of the best estimate  $\hat{\alpha}$  is calculated by finding  $\hat{\alpha}'$ , which satisfies [33]

$$\chi^2(\hat{\alpha}') = \chi_{\text{min}}^2 + n^2. \quad (54)$$

For a 1(2)-parameter fit a  $1\text{-}\sigma$  standard deviation corresponds to a confidence level of 68(39)%.

#### IV. $eeqq$ CONTACT INTERACTIONS

In this section we present the results of our global fit to the  $eeqq$  contact interactions. The HERA data, Tables I and II, mainly constrain the  $eeuu$  and  $eedd$  contact interactions, as do the cesium atom weak charge (26) and the three asymmetries (31), (35), (39) of polarized electron scattering on nuclei targets. The Drell-Yan (DY) lepton-pair production data, Table III, are sensitive to  $eeqq$  and  $\mu\mu qq$  contact interactions mainly of the first generation quarks ( $u$  and  $d$ ). The DY data show no indication of  $e\text{-}\mu$  universality violation, hence we assume the  $e\text{-}\mu$  universality of the contact interactions when we include this data in our fit. The LEP/SLC measurements of  $e^+e^- \rightarrow \text{hadrons}$ , Table IV and Eq. (48) constrain  $eeqq$  contact interactions summed over five flavors of quarks,  $u, d, s, c$  and  $b$ . Since  $b$  and  $c$  flavor-tagging measurements have only limited accuracy, we need to assume quark-flavor universality relations when we include the LEP/SLC data in our global fit,

$$\eta_{\alpha\beta}^{eu} = \eta_{\alpha\beta}^{ec}, \quad \eta_{\alpha\beta}^{ed} = \eta_{\alpha\beta}^{es} = \eta_{\alpha\beta}^{eb}, \quad (55)$$

where  $\alpha\beta = LL, LR, RL, RR$ . Finally, the neutrino-nucleon scattering data (49) constrain the neutral current  $\nu_\mu\nu_\mu uu$  and  $\nu_\mu\nu_\mu dd$  contact interactions. To include neutrino data in the global analysis we need to assume the electroweak gauge symmetry relations of Eq. (4). Our global fits for the  $eeqq$  contact interactions are thereby organized in the increasing order of model dependence.

In Table V we summarize the experimental constraints obtained on the  $eeqq$  contact interactions  $\eta_{\alpha\beta}^{eq}$  in the various “models”: (a) the SM result, (b) the choice  $\eta_{LR}^{eu} = \eta_{RL}^{eu} = 1.4 \text{ GeV}^{-2}$  used in our previous qualitative demonstration of the effects of the contact interactions [8], (c) the fit when all 8  $eeqq$  contact terms are allowed to vary freely, (d) a minimal choice that would explain the HERA and other data, (e) a vector-vector model, (f) an axial vector - axial vector model, and (g) the SU(12) model [9]. The fits were performed using the program MINUIT [44].

The breakdown of the minimum  $\chi^2$  for each model is summarized in Table VI. The SM global-fit is excellent, giving  $\chi^2/\text{d.o.f.} = 176.4/164$ . The SM gives the best  $\chi^2$  of the CDF-DY data. Only for the H1 data does the SM give a poor representation. Our previous choice (b) fits the H1 data but does not fit ZEUS nor CDF-DY data well. For case (c) in which all eight parameters are allowed to vary, the minimization maintains a balance among the  $\chi^2$  of the data sets. From Tables V and VI we see that the best estimate for the  $LR$  and  $RL$  components are similar and the minimum  $\chi^2$  for (c) and (d) also is comparable. This confirms that the HERA anomaly is better explained by  $LR$  and  $RL$  components, which have less influence on other experiments. In the cases (e), (f), and (g) the  $\chi^2$  for the HERA data does not improve over (c) and (d), which indicates that the  $VV$ ,  $AA$ , and the SU(12) chirality combinations cannot better explain the HERA anomaly without upsetting other experiments. Other  $\eta_{\alpha\beta}^{eq}$  solutions could conceivably give a smaller  $\chi^2$  for HERA but only at the expense of larger  $\chi^2$ 's for the other experiments. The above fits in Table V and VI do not include the  $\nu N$  data because most of the “models” do not maintain the SU(2) invariance

relations (3) and (4).

In all the fits, we notice that  $\eta_{LR}^{ed}$  and  $\eta_{RL}^{ed}$  are in general larger than the others, even larger than  $\eta_{LR}^{eu}$  and  $\eta_{RL}^{eu}$ . This is because (i) the excess events at HERA is best explained by the  $LR$  and  $RL$  chiralities (see Eq. (24)), (ii) in Drell-Yan production at the Tevatron  $u\bar{u}$  annihilation dominates over  $d\bar{d}$ , and the Drell-Yan cross sections agree with the SM prediction. Therefore, the minimization process increases  $\eta_{LR}^{ed}$  and  $\eta_{RL}^{ed}$  to fit the HERA data without spoiling the SM fit to the Drell-Yan cross section.

Table VII shows how the best estimates for  $\eta_{\alpha\beta}^{eq}$  parameters change when data sets are added successively in the minimization. The most dramatic changes occur when the data for Drell-Yan (DY) lepton-pair production at the Tevatron are included. Note that when we include the  $\nu$ -N data in the last column of Table VII the  $SU(2)_L$  invariance relations of Eqs. (3) and (4) are assumed and then we have 7 free parameters instead of 8. Table VII shows that the HERA and DY data are not fully compatible. There is an abrupt change of the best-fit  $\eta_{\alpha\beta}^{eq}$  values and a sudden increase of the  $\chi^2$  from the HERA data between the third (HERA+APV+eN) and fourth (HERA+APV+eN+DY) columns. The difference  $\chi_{SM}^2 - \chi_{min}^2$  is as large as 12.8 at the third column but it reduces to 8.2 in the fourth column after including the CDF-DY data, which is no significant improvement over the SM since there are 8  $eeqq$  contact terms allowed to vary freely.

Figure 1 shows the fit for the HERA data and Fig. 2 shows that for the CDF-DY data from the models as given in Table III: (i) fit to HERA only (long-dashed curves), (ii) fit to HERA+APV+eN data (dotted curves), (iii) fit including the DY data assuming  $e$ - $\mu$  universality (dash-dotted curves), (iv) fit including the LEP and  $\nu$ N data, assuming the quark flavor universality and  $SU(2)_L$  invariance relations (dashed curves). The incompatibility of the HERA high- $Q^2$  data and the CDF high mass DY data can be seen in these figures. Even allowing for general  $eeqq$  contact interactions, it is not possible to find a good fit to both the HERA and CDF-DY data.

Finally, we present the result of the global fit to all low and high energy lepton-quark experiments by assuming the flavor universality and the  $SU(2)_L$  invariance of the contact

interactions. We then have the seven independent lepton-quark contact interactions that appear in the last column of Table VII. The errors given for each  $\eta_{\alpha\beta}^{eq}$  are correlated. The correlation matrix as obtained from MINUIT [44] is as follows:

$$\begin{pmatrix} 1.00 & -0.65 & 0.78 & -0.52 & 0.91 & 0.14 & -0.13 \\ -0.65 & 1.00 & -0.76 & 0.69 & -0.38 & -0.31 & 0.47 \\ 0.78 & -0.76 & 1.00 & -0.71 & 0.58 & 0.36 & -0.49 \\ -0.52 & 0.69 & -0.71 & 1.00 & -0.43 & 0.22 & 0.75 \\ 0.91 & -0.38 & 0.58 & -0.43 & 1.00 & -0.18 & -0.10 \\ 0.14 & -0.31 & 0.36 & 0.22 & -0.18 & 1.00 & 0.35 \\ -0.13 & 0.47 & -0.49 & 0.75 & -0.10 & 0.35 & 1.00 \end{pmatrix}, \quad (56)$$

where the row and column indices are labeled in the order:  $\eta_{LL}^{eu}$ ,  $\eta_{LR}^{eu}$ ,  $\eta_{RL}^{eu}$ ,  $\eta_{RR}^{eu}$ ,  $\eta_{LL}^{ed}$ ,  $\eta_{LR}^{ed}$ ,  $\eta_{RR}^{ed}$ . The covariance matrix  $C$  can be formed by  $C_{ij} = \sigma_i \sigma_j \rho_{ij}$ , where  $\sigma_i$  is the error of the  $i$ -th parameter. The eigenvectors of the covariance matrix are constrained as:

$$.386\eta_{LL}^{eu} + .319\eta_{LR}^{eu} - .620\eta_{RL}^{eu} - .293\eta_{RR}^{eu} + .261\eta_{LL}^{ed} + .321\eta_{LR}^{ed} - .329\eta_{RR}^{ed} = 0.034 \pm 0.031, \quad (57a)$$

$$.737\eta_{LL}^{eu} + .131\eta_{LR}^{eu} + .126\eta_{RL}^{eu} + .080\eta_{RR}^{eu} - .630\eta_{LL}^{ed} - .133\eta_{LR}^{ed} + .055\eta_{RR}^{ed} = 0.014 \pm 0.063, \quad (57b)$$

$$.216\eta_{LL}^{eu} - .545\eta_{LR}^{eu} - .232\eta_{RL}^{eu} + .682\eta_{RR}^{eu} + .153\eta_{LL}^{ed} - .014\eta_{LR}^{ed} - .338\eta_{RR}^{ed} = -0.92 \pm 0.29, \quad (57c)$$

$$.035\eta_{LL}^{eu} - .678\eta_{LR}^{eu} - .394\eta_{RL}^{eu} - .473\eta_{RR}^{eu} - .199\eta_{LL}^{ed} - .047\eta_{LR}^{ed} + .343\eta_{RR}^{ed} = -0.45 \pm 0.37, \quad (57d)$$

$$.429\eta_{LL}^{eu} + .041\eta_{LR}^{eu} + .096\eta_{RL}^{eu} + .070\eta_{RR}^{eu} + .638\eta_{LL}^{ed} - .230\eta_{LR}^{ed} + .583\eta_{RR}^{ed} = 0.33 \pm 0.82, \quad (57e)$$

$$.063\eta_{LL}^{eu} - .098\eta_{LR}^{eu} + .187\eta_{RL}^{eu} + .158\eta_{RR}^{eu} - .053\eta_{LL}^{ed} + .904\eta_{LR}^{ed} + .326\eta_{RR}^{ed} = 1.04 \pm 1.46, \quad (57f)$$

$$.268\eta_{LL}^{eu} - .336\eta_{LR}^{eu} + .590\eta_{RL}^{eu} - .434\eta_{RR}^{eu} + .249\eta_{LL}^{ed} + .079\eta_{LR}^{ed} - .459\eta_{RR}^{ed} = -0.36 \pm 1.50. \quad (57g)$$

The strongest constraint (57a) is essentially due to the atomic parity violation experiment and hence it agrees roughly with the result of the corresponding fit to the low energy electroweak data only [36]. The rest of the constraints show significant improvements over those obtained from low energy experiments, even though the analysis of Ref. [36] made a more restrictive assumption that  $\eta_{LL}^{eu} = \eta_{LL}^{ed}$ . The combined effect of low-energy and

high-energy data is that irrespective of the flavor and chirality combination no  $eeqq$  contact interactions can be significantly larger than about  $1 \text{ TeV}^{-2}$ .

## V. CONCLUSIONS

In summary, we have made a general investigation to determine whether the excess of events observed at high- $Q^2$  in the HERA experiments can be understood in terms of contact interactions. All available low and high energy data relevant to  $eeqq$  contact terms have been included in a global fit. Our findings can be summarized as follows:

- (i) If the HERA high  $Q^2$  events are due to  $eeqq$  contact interactions,  $\eta_{LR}^{eu}$  and  $\eta_{RL}^{eu}$  terms are the most effective in explaining the data.
- (ii) The CDF data on high mass Drell-Yan lepton-pair production, however, strongly restrict the  $eeuu$  contact interactions irrespective of their chirality structure.
- (iii) Once the high-energy data and the low-energy electroweak data are combined, all  $eeqq$  contact interactions are strongly constrained and the possibility of explaining the HERA high  $Q^2$  events with contact interactions is limited.
- (iv) The SM gives a reasonably good overall description of all the electron-hadron data, including the HERA high  $Q^2$  events.

## ACKNOWLEDGMENTS

K.C. would like to thank S. Godfrey and K. McFarland for discussions. This research was supported in part by the JSPS-NSF Joint Research Project, in part by the U.S. Department of Energy under Grant Nos. DE-FG03-93ER40757 and DE-FG02-95ER40896 and in part by the University of Wisconsin Research Committee with funds granted by the Wisconsin Alumni Research Foundation.

## REFERENCES

- [1] The H1 Collaboration, C. Adloff et al., report DESY 97-24 [hep-ex/9702012] (1997).
- [2] The ZEUS Collaboration, J. Breitweg et al., report DESY 97-025 [hep-ex/9702015] (1997).
- [3] G. Altarelli, J. Ellis, G.F. Giudice, S. Lola, and M.L. Mangano, report CERN-TH/97-40 [hep-ph/9703276].
- [4] J. Blümlein, hep-ph/9703287; J. Kalinowski, R. Rückl, H. Spiesberger, and P.M. Zerwas, hep-ph/9703288, *Z. Phys.* **C74**, 595 (1997); K.S. Babu, C. Kolda, J. March-Russell, and F. Wilczek, hep-ph/9703299; M. Suzuki, hep-ph/9703316; G.K. Leontaris and J.D. Vergados, hep-ph/9703338; Z. Kunszt and W.J. Stirling, hep-ph/9703427; T. Plehn et al., hep-ph/9703433; D. Friberg, E. Norrbin, and T. Sjöstrand, hep-ph/9704214; I. Montvay, hep-ph/9704280; S.F. King and G.K. Leontaris, hep-ph/9704336; J. Elwood and A. Faraggi, hep-ph/9704363; B. Dutta, R. Mohapatra, and S. Nandi, hep-ph/9704428; S. Jadach, W. Placzek, and B. Ward, hep-ph/9705395; K.S. Babu, C. Kolda, and J. March-Russell, hep-ph/9705414; J. Ellis, S. Lola, and K. Sridhar, hep-ph/9705416; S. Jadach, B.F.L. Ward, and Z. Was, hep-ph/9705429; A. Blumhofer and B. Lampe, hep-ph/9706454; E. Keith and E. Ma, hep-ph/9707214; N.G. Deshpande and B. Dutta, hep-ph/9707274.
- [5] T. Kon and T. Kobayashi, *Phys. Lett.* **B270**, 91 (1991).
- [6] D. Choudhury and S. Raychaudhuri, hep-ph/9702392; H. Dreiner and P. Morawitz, hep-ph/9703279; J. Kalinowski, R. Rückl, H. Spiesberger, and P.M. Zerwas, hep-ph/9703436; T. Kon and T. Kobayashi, hep-ph/9704221; R. Barbieri, A. Strumia, and Z. Berezhiani, hep-ph/9704275; G.F. Giudice and R. Rattazzi, hep-ph/9704339; A.S. Belyaev and A.V. Gladyshev, hep-ph/9704343; J. Kalinowski, hep-ph/9706203; J.E. Kim and P. Ko, hep-ph/9706387; A.S. Joshipura, V. Ravindran, and S.K. Vempati,

- hep-ph/9706482; M. Frank and H. Hamidian, hep-ph/9706510; M. Guchait and D.P. Roy, hep-ph/9707275; T. Kon, T. Matsushita, and T. Kobayashi, hep-ph/9707355.
- [7] S. Adler, hep-ph/9702378; K. Akama, K. Katsuura, and H. Terazawa, hep-ph/9704327.
- [8] V. Barger, K. Cheung, K. Hagiwara, and D. Zeppenfeld, hep-ph/9703311, Phys. Lett. **B** (in press).
- [9] A. Nelson, hep-ph/9703379, Phys. Rev. Lett. **78**, 4159 (1997).
- [10] N. Bartolomeo and M. Fabbrichesi, hep-ph/9703375.
- [11] W. Buchmüller and D. Wyler, hep-ph/9704317.
- [12] N.G. Deshpande, B. Dutta, and Xiao-Gang He, preprint OITS-630 [hep-ph/9705236].
- [13] M.C. Gonzalez-Garcia and S.F. Novaes, hep-ph/9703346; S. Godfrey, hep-ph/9704380; L. Giusti and A. Strumia, hep-ph/9706298; Z. Cao, X.-G. He, and B. McKellar, hep-ph/9707227; F. Cornet and J. Rico, hep-ph/9707229.
- [14] S. Kuhlmann, H.L. Lai, and W.K. Tung, hep-ph/9704338; K.S. Babu, C. Kolda, and J. March-Russell, hep-ph/9705399; J.F. Gunion and R. Vogt, hep-ph/9706252.
- [15] M. Drees, hep-ph/9703332; U. Bassler and G. Bernardi, hep-ph/9707024.
- [16] H. Kambara for the CDF Collaboration, talk given at *Hadron Collider Physics XII*, Stony Brook, June 5–11, 1997.
- [17] D. Norman for the D0 Collaboration, talk given at *Hadron Collider Physics XII*, Stony Brook, June 5–11, 1997.
- [18] C.S. Wood et al., Science **275**, 1759 (1997).
- [19] C.Y. Prescott et al., Phys. Lett. **B84**, 524 (1979).
- [20] W. Heil et al., Nucl. Phys. **B327**, 1 (1989).

- [21] P.A. Souder et al., Phys. Rev. Lett. **65**, 694 (1990).
- [22] A. Bodek for the CDF Collaboration, preprint Fermilab-Conf-96/341-E (1996); also new data found at <http://www-cdf.fnal.gov/physics/ewk/dy.html>. In our analysis, we used the data from the above web-page.
- [23] LEP Collaborations and SLD Collaboration, “A Combination of Preliminary Electroweak Measurements and Constrains on the Standard Model”, prepared from contributions to the 28th International Conference on High Energy Physics, Warsaw, Poland, CERN-PPE/96-183 (Dec. 1996).
- [24] OPAL Collaboration, G. Alexander et al., Phys. Lett. **B376**, 232 (1996); *ibid* **B387**, 432 (1996); *ibid* **B391**, 221 (1996).
- [25] L3 Collaboration, Phys. Lett. **B370**, 195 (1996); CERN-PPE/97-XX, L3 preprint 117 (May 1997).
- [26] ALEPH Collaboration, Phys. Lett. **B378**, 373 (1996).
- [27] P. Langacker and J. Erler, presented at the Ringberg Workshop on the Higgs Puzzle, Ringberg, Germany, 12/96, hep-ph/9703428.
- [28] K.S. McFarland et al. (CCFR), FNAL-Pub-97/001-E, hep-ex/9701010.
- [29] E. Eichten, K. Lane, and M. Peskin, Phys. Rev. Lett. **50**, 811 (1982).
- [30] R.J. Cashmore et al., Phys. Rev. **122**, 275 (1985); R. Rückl, Phys. Lett. **B129**, 363 (1983); Nucl. Phys. **B234**, 91 (1984).
- [31] P. Chiapetta and J.-M. Virey, Phys. Lett. **B389**, 89 (1996).
- [32] W. Buchmüller and D. Wyler, Nucl. Phys. **B268**, 621 (1986).
- [33] Review of Particle Properties, Phys. Rev. **D54**, 1 (1996).
- [34] W. Buchmüller, R. Rückl, and D. Wyler, Phys. Lett. **B191**, 442 (1987); J. Hewett and

- T. Rizzo, hep-ph/9703337.
- [35] P. Langacker, M. Luo, and A. Mann, Rev. Mod. Phys. **64**, 87 (1992).
- [36] G.-C. Cho, K. Hagiwara and S. Matsumoto, hep-ph/9707334.
- [37] K. Hagiwara, D. Haidt, C.S. Kim and S. Matsumoto, Z. Phys. **C64**, 559 (1994); Errata **C 68**, 352 (1995).
- [38] D.H. Beck, Phys. Rev. **D39**, 3248 (1987).
- [39] H. Burkhardt and B. Pietrzyk, Phys. Lett. **B356**, 398 (1995).
- [40] V. Barger and R.J.N. Phillips, *Collider Physics*, (Addison-Wesely, Reading MA, updated edition 1996).
- [41] S.G. Gorishny, A. Kataev, and S.A. Larin, Phys. Lett. **B259**, 114 (1991); L.R. Surguladze and M.A. Samuel, Phys. Rev. Lett. **66**, 560 (1991).
- [42] G. Fogli and D. Haidt, Z. Phys. **C40**, 379 (1988).
- [43] A. Blondel et al. (CDHS), Z. Phys. **C45**, 361 (1990); J.V. Allaby et al. (CHARM), Z. Phys. **C36**, 611 (1987); D. Allasia et al. (BEBC), Nucl. Phys. **B307**, 1 (1988); C.G. Arroyo et al. (CCFR), Phys. Rev. Lett. **72**, 3452 (1994).
- [44] CERN Program Library entry D506.

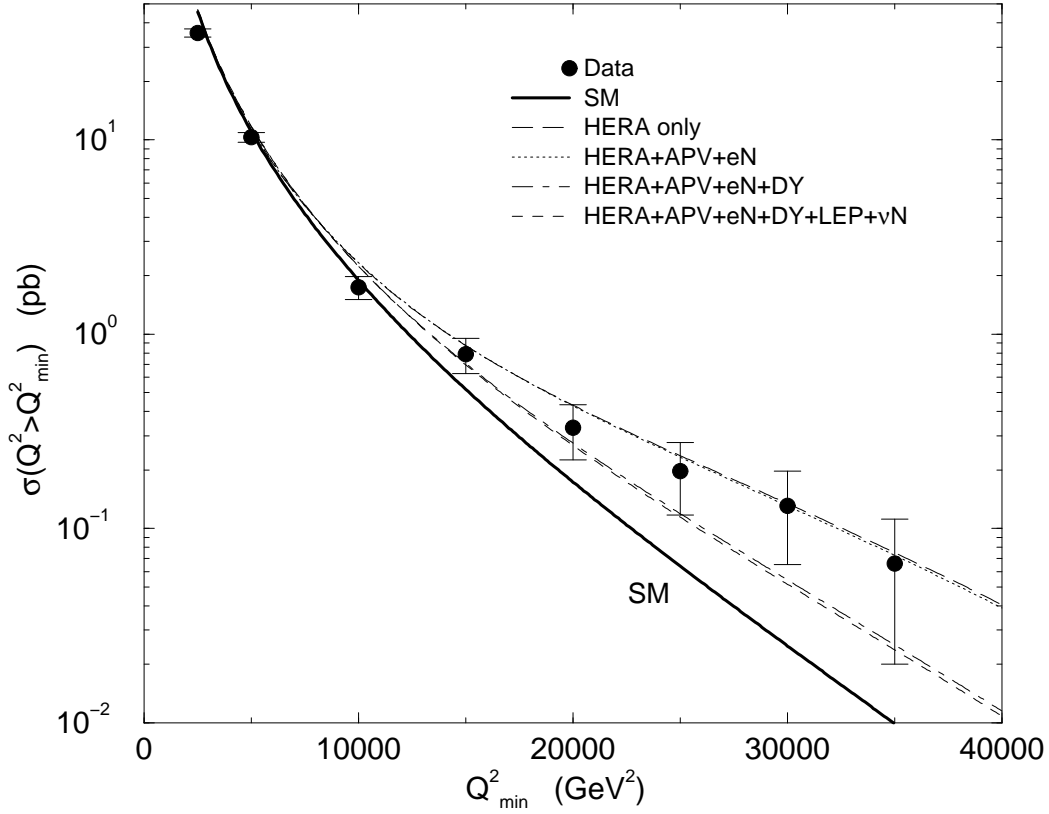


FIG. 1. Integrated cross sections for  $e^+p \rightarrow e^+X$  versus a minimum  $Q^2$  for the SM (solid curve) and for four choices of contact interactions: best-fit for the H1 and ZEUS data (long-dashed curve), best-fit including the low energy electron-quark coupling measurements (dotted curve), best-fit further including the Tevatron lepton-pair production data (dot-dashed curve), and the best-fit including also the LEP data and the neutrino-scattering data (dashed curve); see Table VII. The data points correspond to combined H1 [1] and ZEUS [2] measurements, assuming constant detection efficiencies of 80% and 81.5%, respectively. Our fits are performed directly on the published data [1,2] as summarized in Tables I and II.

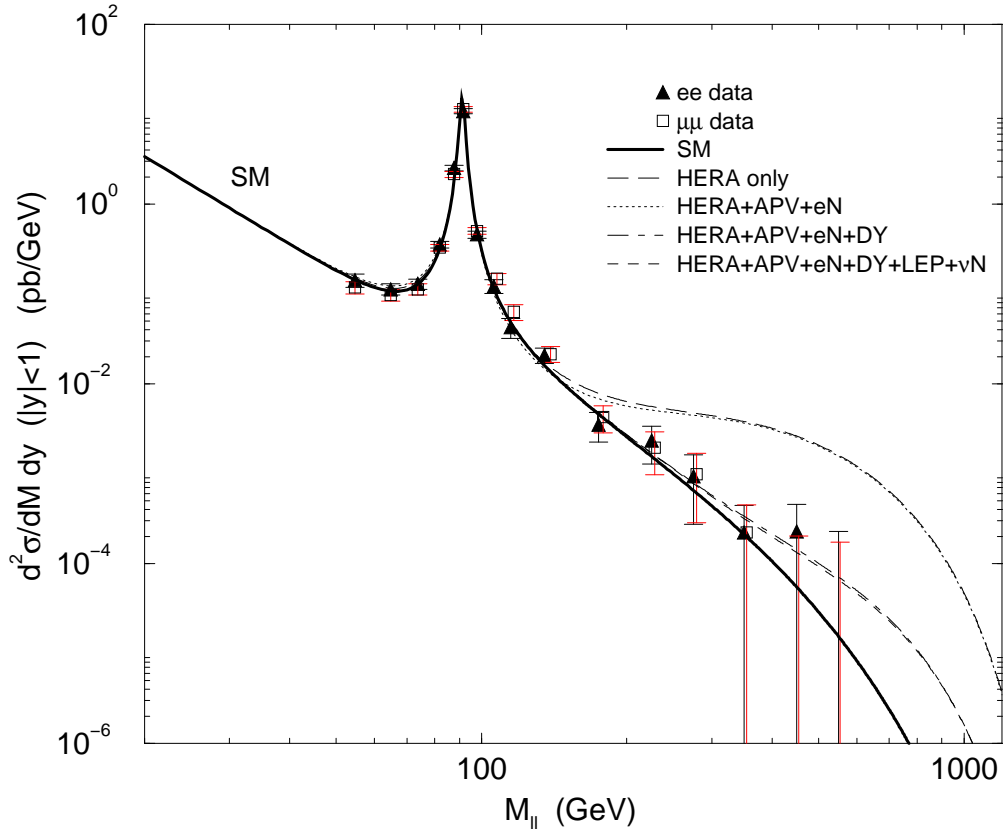


FIG. 2. The Drell-Yan cross section  $\bar{p}p \rightarrow (\mu^+\mu^- \text{ or } e^+e^-)X$  at the Tevatron ( $\sqrt{s} = 1.8$  TeV) for the SM (solid curve) and the four choices of contact interactions as in Fig. 1. Preliminary CDF data [23] are shown separately for  $e^+e^-$  (solid triangle) and  $\mu^+\mu^-$  (open square) pair; see Table III. The cross section is averaged over  $y$  as  $\frac{1}{2} \int_{-1}^1 dy \frac{d^2\sigma}{dM dy}$ .

TABLE I. The expected and observed numbers of events in each bin of the  $x - y$  plane from ZEUS. The expected number is listed above the observed number.

$x_{\min}$	0.05	0.15	0.25	0.35	0.45	0.55	0.65	0.75	0.85
$x_{\max}$	0.15	0.25	0.35	0.45	0.55	0.65	0.75	0.85	0.95
$0.85 < y < 0.95$	8.8 9	1.2 3	0.32	0.10	0.028 1	0.01	0.0034		
$0.75 < y < 0.85$	12 16	2.5 4	0.50 1	0.15	0.050	0.011	0.0039		
$0.65 < y < 0.75$	13 10	3.7 3	0.86	0.26	0.082	0.022	0.0054 1	0.0020	
$0.55 < y < 0.65$	15 12	6.1 3	1.65 3	0.46 1	0.15	0.046	0.0090	0.0024	
$0.45 < y < 0.55$	12 6	11 13	2.5 1	0.85	0.28	0.084 1	0.0208	0.0032	
$0.35 < y < 0.45$	4.6 3	18 17	5.5 6	1.75	0.52	0.16	0.0403	0.0093	
$0.25 < y < 0.35$		18 23	11 6	3.74 7	1.19 1	0.34 2	0.1104	0.0175	0.0066
$0.15 < y < 0.25$		2.2 1	14 15	9.6 10	3.32 3	1.2	0.2784 1	0.0717	0.0077
$0.05 < y < 0.15$				1.3 1	2.14 3	1.6 2	0.9052 1	0.3022 1	0.1216

TABLE II. The expected and observed numbers of events in each bin of the  $x - y$  plane from H1. The expected number is listed above the observed number.

$x_{\min}$	0.06236	0.2494	0.3395	0.3592	0.3794	0.4002	0.4216	0.4435
$x_{\max}$	0.2494	0.3395	0.3592	0.3794	0.4002	0.4216	0.4435	0.95
$0.5 < y < 0.9$	73.59	2.2	0.27	0.21	0.15	0.15	0.14	0.39
	76	3	0	0	1	0	1	3
$0.4 < y < 0.5$	56.28	2.28	0.25	0.21	0.19	0.07	0.08	0.24
	59	2	0	0	0	1	1	0
$0.3 < y < 0.4$	65.13	3.77	0.40	0.42	0.36	0.24	0.19	0.69
	80	3	1	1	0	0	0	0
$0.2 < y < 0.3$	70.9	9.93	1.05	0.91	0.75	0.61	1.45	1.4
	64	12	2	0	1	1	0	1

TABLE III. Preliminary CDF Drell-Yan Data extracted from their figures. Both  $e^+e^-$  and  $\mu^+\mu^-$  samples are shown. The data is the  $y$ -averaged integrated cross section  $\frac{1}{2} \int_{-1}^1 dy \frac{d^2\sigma}{dMdy}$ .

$M_{ee}(\text{GeV})$	$\frac{1}{2} \int_{-1}^1 dy \frac{d^2\sigma}{dMdy} (\text{pb/GeV})$	$M_{\mu\mu}(\text{GeV})$	$\frac{1}{2} \int_{-1}^1 dy \frac{d^2\sigma}{dMdy} (\text{pb/GeV})$
54.63	$0.142^{+0.024}_{-0.023}$	54.63	$0.118 \pm 0.019$
64.90	$0.113^{+0.017}_{-0.016}$	64.90	$0.098^{+0.015}_{-0.014}$
73.82	$0.130^{+0.016}_{-0.017}$	73.82	$0.113^{+0.017}_{-0.016}$
81.86	$0.358^{+0.029}_{-0.035}$	81.86	$0.329^{+0.029}_{-0.030}$
87.66	$2.537^{+0.168}_{-0.188}$	87.66	$2.162^{+0.158}_{-0.173}$
91.68	$10.779^{+0.861}_{-0.668}$	91.68	$11.345^{+0.906}_{-0.839}$
97.92	$0.462^{+0.037}_{-0.045}$	97.92	$0.502^{+0.044}_{-0.040}$
105.96	$0.122^{+0.022}_{-0.020}$	107.74	$0.148^{+0.020}_{-0.021}$
114.88	$0.0427^{+0.0104}_{-0.0105}$	116.67	$0.0635^{+0.0125}_{-0.0131}$
134.97	$0.0209 \pm 0.0041$	138.98	$0.0214^{+0.0045}_{-0.0042}$
174.69	$0.00352 \pm 0.00127$	178.71	$0.00426^{+0.0015}_{-0.0014}$
225.11	$0.00234 \pm 0.00105$	228.69	$0.00195^{+0.00099}_{-0.00097}$
275.11	$(9.41 \pm 6.70) \times 10^{-4}$	279.13	$(9.91 \pm 7.05) \times 10^{-4}$
350.09	$(2.22^{+2.21}_{-2.22}) \times 10^{-4}$	354.11	$(2.22^{+2.26}_{-2.22}) \times 10^{-4}$
450.06	$(2.27 \pm 2.27) \times 10^{-4}$	454.08	$(0.0^{+2.03}_{-0.0}) \times 10^{-4}$
550.04	$(0.0^{+2.27}_{-0.0}) \times 10^{-4}$	554.06	$(0.0^{+1.74}_{-0.0}) \times 10^{-4}$

TABLE IV. Table showing the LEP1 and SLD data, and LEP1.5 and LEP2 data that are relevant to our analysis [23–27].

$E_{CM}$	$\sigma_{\text{had}}$	$\sigma_{\text{had}}^{\text{SM}}$
LEP1, SLD : $\sqrt{s} = M_Z$	$41.508 \pm 0.056$ nb	41.465 nb
OPAL : $\sqrt{s} = 130.26$ GeV	$66 \pm 5 \pm 3$ pb	78 pb
OPAL : $\sqrt{s} = 136.23$ GeV	$60 \pm 5 \pm 2$ pb	63 pb
OPAL : $\sqrt{s} = 140$ GeV	$50 \pm 36 \pm 2$ pb	56 pb
L3 : $\sqrt{s} = 130.3$ GeV	$81.8 \pm 6.4$ pb	78 pb
L3 : $\sqrt{s} = 136.3$ GeV	$70.5 \pm 6.2$ pb	64 pb
L3 : $\sqrt{s} = 140.2$ GeV	$67 \pm 47$ pb	56 pb
ALEPH : $\sqrt{s} = 130$ GeV	$74.2 \pm 5.2 \pm 3.3$ pb	76.9 pb
ALEPH : $\sqrt{s} = 136$ GeV	$57.4 \pm 4.5 \pm 1.8$ pb	62.5 pb
OPAL : $\sqrt{s} = 161.3$ GeV	$35.3 \pm 2.0 \pm 0.7$ pb	33.2 pb
L3 : $\sqrt{s} = 161.3$ GeV	$37.3 \pm 2.2$ pb	34.9 pb
L3 : $\sqrt{s} = 170.3$ GeV	$39.5 \pm 7.5$ pb	29.8 pb
L3 : $\sqrt{s} = 172.3$ GeV	$28.2 \pm 2.2$ pb	28.9 pb

TABLE V. The best estimate of the contact interaction parameters  $\eta_{\alpha\beta}^{eq}$  and the corresponding  $\chi^2_{\min}$  for (c) all eight  $\eta_{\alpha\beta}^{eq}$  being free, and (d)–(f) various chirality combinations. The  $\chi^2$  for the Standard Model and the “eye-ball” solution from our previous paper are shown in (a) and (b), respectively. The data sets included are: H1, ZEUS, APV,  $e$ -N, DY, and LEP. The number of degree of freedom for the Standard Model is 164.

Chirality Combination	Best estimate (unit=TeV <sup>-2</sup> )	$\chi^2_{\min}$
(a) Standard Model		176.4/164 d.o.f.
(b) $\eta_{LR}^{eu} = \eta_{RL}^{eu} = 1.4\text{TeV}^{-2}$ , others=0		187.1/163 d.o.f.
(c) All free	$\eta_{LL}^{eu} = 0.16^{+0.61}_{-0.48}$ , $\eta_{RR}^{eu} = -0.001^{+0.63}_{-0.55}$ , $\eta_{LR}^{eu} = 0.80^{+0.46}_{-0.62}$ , $\eta_{RL}^{eu} = 0.19^{+0.65}_{-0.71}$ , $\eta_{LL}^{ed} = 0.31^{+0.92}_{-1.01}$ , $\eta_{RR}^{ed} = 0.62^{+0.98}_{-1.09}$ , $\eta_{LR}^{ed} = 1.66^{+1.18}_{-1.66}$ , $\eta_{RL}^{ed} = 1.95^{+1.10}_{-1.63}$ ,	167.2/156 d.o.f.
(d) $\eta_{RL}^{eu} = \eta_{LR}^{eu}$ , $\eta_{RL}^{ed} = \eta_{LR}^{ed}$ , others=0	$\eta_{RL}^{eu} = \eta_{LR}^{eu} = 0.51^{+0.26}_{-0.27}$ , $\eta_{RL}^{ed} = \eta_{LR}^{ed} = 1.97^{+0.50}_{-0.70}$ ,	170.0/ 162 d.o.f.
(e) $\eta_{VV}^{eu}, \eta_{VV}^{ed}$	$\eta_{VV}^{eu} = 0.47^{+0.20}_{-0.23}$ , $\eta_{VV}^{ed} = 1.10^{+0.28}_{-0.38}$	172.5/162 d.o.f.
(f) $\eta_{AA}^{eu}, \eta_{AA}^{ed}$	$\eta_{AA}^{eu} = -0.36^{+0.17}_{-0.14}$ , $\eta_{AA}^{ed} = -0.36^{+0.44}_{-0.46}$	173.0 /162 d.o.f.
(g) SU(12)	$\eta_{LL}^{eu} = -\eta_{LR}^{eu} = -0.39^{+0.68}_{-0.31}$ , $\eta_{RL}^{eu} = -\eta_{RR}^{eu} = 0.29^{+0.48}_{-0.68}$ , $\eta_{LL}^{ed} = -\eta_{LR}^{ed} = -0.81^{+1.23}_{-0.96}$ , $\eta_{RL}^{ed} = -\eta_{RR}^{ed} = -0.11^{+1.24}_{-0.92}$	172.7/160 d.o.f.

TABLE VI. Breakdown of the minimum  $\chi^2$  by experiment for the models in Table V.

# Data points	H1	ZEUS	APV	eN	CDF-DY	LEP
	32	81	1	4	32	14
(a) SM	33.9	59.9	1.2	1.8	62.2	17.4
(b) $\eta_{LR}^{eu} = \eta_{RL}^{eu} = 1.4\text{TeV}^{-2}$ , others=0	29.0	66.5	1.2	1.8	70.9	17.7
(c) All free	29.9	58.1	0.0	0.5	62.6	16.1
(d) $\eta_{RL}^{eu} = \eta_{LR}^{eu} = 0.51$ , $\eta_{RL}^{ed} = \eta_{LR}^{ed} = 1.97$	30.0	58.2	1.2	1.8	62.7	16.1
(e) $\eta_{VV}^{eu} = 0.47, \eta_{VV}^{ed} = 1.10$	30.4	58.7	1.2	1.8	63.1	17.4
(f) $\eta_{AA}^{eu} = -0.36, \eta_{AA}^{ed} = -0.36$	31.9	58.8	1.2	1.8	62.2	17.1
(g) $\eta_{LL}^{eu} = -\eta_{LR}^{eu} = -0.39$ , $\eta_{RL}^{eu} = -\eta_{RR}^{eu} = 0.29$ , $\eta_{LL}^{ed} = -\eta_{LR}^{ed} = -0.81$ , $\eta_{RL}^{ed} = -\eta_{RR}^{ed} = -0.11$	32.0	58.8	1.2	1.5	62.3	17.0

TABLE VII. The best estimate of the  $\eta_{\alpha\beta}^{eq}$  parameters when various data sets are added successively. In the last column when the  $\nu$ -N data are included the  $\eta_{L\beta}^{\nu q}$  are given in terms of  $\eta_{L\beta}^{eq}$  by Eq. (4), we assume  $\eta_{RL}^{eu} = \eta_{RL}^{ed}$  in the last column.

	HERA only	HERA+APV	HERA+APV +eN	HERA+APV +eN+DY	HERA+APV +eN+DY+LEP	HERA+DY+APV +eN+LEP+ $\nu$ N
$\eta_{LL}^{eu}$	$0.38^{+4.10}_{-6.04}$	$0.69^{+3.65}_{-5.49}$	$0.49^{+2.90}_{-2.99}$	$0.16^{+0.67}_{-0.53}$	$0.16^{+0.61}_{-0.48}$	$-0.082^{+0.67}_{-0.40}$
$\eta_{LR}^{eu}$	$-4.93^{+2.81}_{-0.96}$	$-4.90^{+6.41}_{-9.72}$	$-2.24^{+4.06}_{-2.90}$	$0.88^{+0.43}_{-0.64}$	$0.80^{+0.46}_{-0.62}$	$0.86^{+0.42}_{-0.73}$
$\eta_{RL}^{eu}$	$-0.14^{+3.29}_{-5.07}$	$-0.39^{+3.52}_{-4.80}$	$-4.20^{+4.51}_{-1.08}$	$0.21^{+0.68}_{-0.78}$	$0.19^{+0.65}_{-0.71}$	$0.38^{+0.67}_{-0.91}$
$\eta_{RR}^{eu}$	$1.28^{+4.42}_{-6.31}$	$1.03^{+4.45}_{-5.90}$	$1.46^{+1.73}_{-3.73}$	$0.011^{+0.65}_{-0.61}$	$-0.0010^{+0.63}_{-0.55}$	$-0.074^{+0.74}_{-0.57}$
$\eta_{LL}^{ed}$	$-2.51^{+10.49}_{-8.24}$	$-1.88^{+8.97}_{-7.59}$	$-4.03^{+7.45}_{-4.09}$	$0.71^{+1.38}_{-1.59}$	$0.31^{+0.92}_{-1.01}$	$0.015^{+0.88}_{-0.52}$
$\eta_{LR}^{ed}$	$-1.42^{+7.40}_{-4.87}$	$-1.19^{+7.04}_{-4.95}$	$-1.97^{+5.87}_{-3.77}$	$1.15^{+1.38}_{-1.99}$	$1.66^{+1.18}_{-1.66}$	$0.88^{+1.06}_{-1.82}$
$\eta_{RL}^{ed}$	$-2.80^{+7.39}_{-5.16}$	$-3.34^{+7.23}_{-4.31}$	$-2.80^{+5.99}_{-2.65}$	$1.50^{+1.29}_{-1.97}$	$1.95^{+1.10}_{-1.63}$	$= \eta_{RL}^{eu}$
$\eta_{RR}^{ed}$	$-3.16^{+10.85}_{-9.18}$	$-4.13^{+9.20}_{-6.43}$	$-2.40^{+7.63}_{-5.48}$	$1.01^{+1.31}_{-1.57}$	$0.62^{+0.98}_{-1.09}$	$0.84^{+0.85}_{-1.11}$
HERA	83.4	83.4	83.6	88.1	88.0	88.6
APV		0.0	0.0	0.001	0.0	0.001
eN			0.38	0.47	0.47	0.67
DY				62.3	62.6	62.2
LEP					16.1	17.1
$\nu$ N						0.007
Total $\chi^2$	83.4	83.4	84.0	150.8	167.2	168.7
SM $\chi^2$	93.8	95.0	96.8	159.0	176.4	176.4
SM d.o.f.	113	114	118	150	164	165